1 **THREE-DIMENSIONAL GEOMETRY OF THE NARWHAL (*MONODON***

2 ***MONOCEROS*) FLUKES IN RELATION TO HYDRODYNAMICS**

3

4 JANET E. FONTANELLA

5 Department of Biology,

6 West Chester University,

7 West Chester, Pennsylvania 19383, U.S.A.

8

9 FRANK E. FISH

10 Department of Biology,

11 West Chester University,

12 West Chester, Pennsylvania 19383, U.S.A.

13

14 NATALIA RYBCZYNSKI

15 Canadian Museum of Nature,

16 Ottawa, Ontario K1P 6P4, Canada

17

18 MARTIN T. NWEEIA

19 Harvard University

20 School of Dental Medicine

21 Boston, Massachusetts 02115, U.S.A.,

22 Smithsonian Institution

23 Washington, D. C. 20227, U. S. A.

24

25   DARLENE R. KETTEN

26   Biology Department

27   Woods Hole Oceanographic Institution,

28   Woods Hole, MA 02543 U.S.A.

29   Department of Otology and Laryngology,

30   Harvard Medical School,

31   Boston, Massachusetts 02114, U.S.A.

32

34

35   Cetaceans (whales, porpoises, and dolphins) use only their flukes for propulsion. Flukes

36   are distally located extensions of the tail, and from a biomechanical standpoint, function as a pair

37   of wings (Vogel 1994). Flukes function to produce thrust generated as an anteriorly directed lift

38   force as flukes oscillate vertically (Fish 1998 a,b). Their cross-sections resemble hydrofoils. For

39   a hydrofoil to be effective, a large lift must be produced while drag is minimized; this, in turn,

40   increases the thrust generated (Weihs 1989; Vogel 1994).

41   The hydrodynamic implications of fluke design can be studied by examining the cross-

42   sections (*i.e.*, parasagittal) of the flukes. Cross-section profiles taken along the horizontal axis

43   exhibit what is a typical streamlined hydrofoil profile with a rounded leading edge and a long,

44   tapered trailing edge. This shape is critical for the generation of lift for thrust, while minimizing

45   induced drag (*i.e.*, drag due to lift production; Lighthill 1970; Vogel 1994). The flukes are

46   symmetrical about the chord (Lang 1966; Bose et al. 1990). The cross-sectional profile of the

47 flukes is similar to symmetrical engineered foils (Fish 1998b). The similarity to engineered foils

48 would imply that cetacean flukes would be capable of effectively generating large lift with low

49 drag at higher angles of attack.

50   The typical planform shape of cetacean flukes is characterized as a tapered wing with

51 sweepback (*i.e.*, rearward inclination of the leading edge). Such a wing shape can achieve

52 improved efficiency by reducing induced drag by 8.8% compared to a wing with an elliptical

53 planform (van Dam 1987). Minimal induced drag occurs in swept wings with a triangular

54 planform approximating the design of most cetacean flukes (Chopra and Kambe 1977; Fish

55 1998b). Aspect ratio (*AR*) measures the relationship between the span and planform area of a

56 hydrofoil and is related to the effectiveness of the hydrofoil's design. A low *AR* is characterized

57 as a short, broad wing, whereas a high *AR* wing is long and narrow. A combination of low sweep

58 with high *AR* allows for high-efficiency rapid swimming, whereas high sweep may compensate

59 for the reduced lift production of low-*AR* flukes (Azuma 1983; Liu and Bose 1993). Highly

60 swept, low-*AR* wings produce maximum lift when operating at high angles of attack, when low-

61 sweep, high-*AR* designs would fail (Hurt 1965). This feature aids in the maintenance of high

62 efficiency at slow, sustained speeds (Magnuson 1978), as observed in *Monodon monoceros*, the

63 narwhal. In general, narwhals are regarded as very slow swimmers that seldom exceed speeds of

64 1.7 m s^{-1} (Minasian *et al*. 1984). Although increasing efficiency, the high sweep angle will

65 reduce thrust. Maintenance of thrust would be facilitated by a higher *AR* hydrofoil planform.

66   The external morphology of flukes is generally considered constant among the Cetacea.

67 An acute departure from the typical fluke shape is found in the narwhal. Narwhals are regionally

68 circumscribed cetaceans that inhabit the Arctic Ocean Atlantic sector (Heide-Jørgensen 2009).

69 They are widely distributed in the ice-packed stretches of waters bordering Greenland and the

70 Canadian High Arctic (Laidre *et al*. 2003). The flukes of mature male narwhals have a slightly

71 concave leading edge without sweepback (Fig. 1; Hay and Mansfield 1989). A female narwhal

72 generally has a fluke very similar in shape to that of a dolphin, which is swept back (Fig. 1).

73 Whether or not the differing fluke morphology is an evolved adaptation that coincides with the

74 long, tapering tusk present on most males is unknown (Fish *et al.* 2007).

75   In this study, we compared the fluke geometries of male and female narwhals, which may

76 be associated with hydrodynamic effects. CT (Computerized tomography) scanning was used to

77 obtain data for analyses of the three-dimensional geometry of the flukes.

78   The flukes from four narwhals (two males and two females) were obtained from

79 aboriginal hunters in the vicinity of Broughton Island, Canada. The body lengths of the animals

80 ranged from 2.98-3.60 m (Table 1). Both males had erupted, upper left tusks. Standard body

81 measurements were made including the span of the fluke (*i.e*., linear distance between fluke

82 tips).

83   The flukes were frozen and shipped to the Canadian Museum of Nature in Ottawa,

84 Canada. The frozen flukes were later transported to the Woods Hole Oceanographic Institution

85 CT imaging facility for scanning. The flukes were placed flat, dorsal side up, on the scanner

86 table, stabilized with plastic wedges and Styrofoam sheets, and scanned tip to tip with span-wise

87 parasagittal cross-sections.

88   CT scans were obtained on a Siemens Volume Zoom CT scanner. Spiral protocols for

89 data acquisition with 0.5- to 1.0-mm detector collimation at 1 mm/sec table feeds were used. All

90 images were reconstructed in both soft tissue and ultra-high resolution kernels with extended

91 attenuation scales to improve discrimination of high density elements. Images were obtained in

92 DICOM formats, and for some data, were reconstructed at 100-μ slice intervals that provide 100

93   μ isotropic voxels needed for finer grain structural analyses. With these parameters, the

94   maximum in-plane resolution was 0.35 mm at 2% of the modulation transfer function. Prior

95   studies suggest 25 μ in-plane pixel resolutions are possible, but a conservative nominal

96   resolution is 50 μ.

97   Because true data base magnifications cannot be obtained from enlargements of

98   processed image files, raw attenuation data were archived onto magneto-optical disks for all

99   scans in order to allow additional post-scan processing as needed.   Image files were archived in

100   DICOM format and 512 matrices on CD. The DICOM images of fluke cross-sections were

101   analyzed using OsiriX (OsiriX Foundation, Geneva, Switzerland, version 2.7.5). A total of 2,715

102   fluke cross-sections were examined for all four specimens; this figure excludes the tailstock

103   cross-sections, for which leading and trailing edges of the flukes were not visible.

104   Measurements of the fluke planforms (Fig. 2) included the span (*FS*; distance from fluke

105   tip to fluke tip), fluke blade span (*BS*, distance from root fluke chord; *RC*, to tip of fluke),

106   planform area (*F$_a$*; total planar area of flukes on the dorsal surface), and sweepback (Λ). *RC* is

107   the chord at the intersection of the fluke blade and the tailstock. The sweepback was measured as

108   the angle between a line extending from 25% of the fluke chord extending from the cranial end

109   of *RC* and to the maximum lateral extension of the fluke tip and a line perpendicular to *RC* (Hurt

110   1965, Fish 1998a, b). The aspect ratio (*AR*) of each fluke was calculated as FS^2/F_a.

111   Measurements of fluke sections for each CT slice (Fig. 2) were made for the chord length

112   (*C*), maximum thickness (*T*), shoulder (*S*), and leading edge radius (*LER*) (Fish *et al*. 2006,

113   2007). *C* was measured as the linear distance from the leading to trailing edge of the fluke. *T* was

114   the maximum vertical distance between the upper and lower side of the fluke perpendicular to

115   the chord line. *S* was measured as the distance from the leading edge to the maximum thickness

116   line. For comparison of narwhals of different sizes, *C*, *T*, and *S* measurements were presented as

117   a percentage of *BS*, starting at 0% at *RC* to 100% at the fluke tip. Leading edge radius (*LER*) was

118   the radius of the curvature of the leading edge as determined from the radius of a circle that

119   connects tangential points of the leading edge and the upper and lower surfaces of the cross-

120   section (Hurt 1965). A circle template was used on images taken at 50% of the *BS* on the two

121   flukes for each individual narwhal to determine radius of the leading edge. *LER* was presented as

122   a proportion of *C* (Fish *et al*. 2007).

123   The thickness ratio ($TR = T / C$) and shoulder position ($SP = S / C$) of each cross section

124   were used as indicators of flow structure and the hydrodynamic performance relating to the

125   generation of lift and drag for foils (von Mises 1945; Hoerner 1965).

126   Microsoft Excel 2004 and KaleidaGraph (Synergy Software, version 4.03) were used to

127   statistically and graphically analyze the data collected. Because of differences in fluke sizes of

128   the individual narwhals, comparisons were made using means (± one standard deviation). The

129   linear measurements from each CT slice (*C*, *T*, *S*) were averaged for the corresponding slice for

130   each fluke blade for an individual animal. The mean values of each measurement and

131   morphological parameter were calculated for each sex. The small sample size precluded

132   statistical analysis beyond descriptive statistics.

133   The *FS* and F_a were both greater for the male narwhals, due to their larger size. The

134   calculated values for aspect ratio did not show significant differences for male and female

135   narwhals. The main difference was the difference in Λ between the sexes (Table 1; Fig. 1).

136   Females had a mean sweepback angle of 31.4 ± 3.3 degrees and males had mean sweepback

137   angles of 20.5 ± 5.2 degrees.

138   It was noted that male N0004 was slightly immature, judging by its overall smaller body

139   size and tusk and the fluke morphology was slightly swept back. Measurements of the *S* for

140   female N0001 were lower than expected at approximately 15% of span (Figs. 3, 5) because of

141   depressions on the ventral side of the cross-sections.

142   For both sexes, the fluke cross-sections were highly streamlined, having a rounded

143   leading edge and a tapering, trailing edge; fluke sections were also symmetrical about the chord

144   (Fig. 2). Both right and left fluke blades were apparently symmetrical. From the root of the fluke,

145   *C, T,* and *S* showed an approximately linear decrease to about 95% of span in which these

146   measurements decreased more rapidly toward the tip (Fig. 3). Differences between male and

147   female narwhals for *C, T,* and *S* were only observed near the fluke root. Interestingly, there was

148   no discernable difference in sectional values for *C* between males and females despite the

149   difference in Λ (Fig. 3).

150   *TR* decreased proximally toward the tailstock (Fig. 4). The maximum values of *TR*

151   occurred at the fluke tip. Over the fluke span, males had a mean *TR* of 0.23 ± 0.02, whereas the

152   females had a mean *TR* of 0.24 ± 0.02. Differences in *TR* between male and female narwhals

153   were apparent from 20% to 90% of *BS*. Within this range, *TR* for females was 5% greater than

154   for the males.

155   *SP* had a U-shaped distribution along the fluke blade span with the highest values at the

156   tip and root of the flukes and lowest at approximately midspan (Fig. 5). Between 20% and 65%

157   of span, males and females had means for *SP* of 0.28 ± 0.00 and 0.30 ± 0.01, respectively. Over

158   this range of span the females averaged a 10% greater *SP* than males.

159   No apparent difference of *LER* was found between males and females. Mean *LER* values

160   were 0.05 ± 0.01 and 0.05 ± 0.00 for males and females, respectively.

161   The general morphology of cetacean flukes influences the requirements of energy for

162   swimming. A highly streamlined fluke is characterized by the symmetrical nature of the cross-

163   sections in the sagittal plane. A rounded leading edge and a tapering, trailing edge are

164   characteristics shown in the cross-sections that are fundamental in the generation of lift, while

165   also reducing drag (Webb 1975, Vogel 1994).

166   The parameters *TR* and *SP* influence the pressure distribution of flow over the surface of

167   the flukes. A favorable gradient has pressure decreasing in the downstream direction, which aids

168   in flow over the fluke surface. An unfavorable gradient has pressure increasing in the

169   downstream direction. This ultimately delays the flow over the fluke's surface. The favorable

170   and unfavorable pressure gradients are located upstream and downstream of *SP,* respectively

171   (Fish 2007). An increase in drag results from an unfavorable pressure gradient, because flow will

172   tend to separate from the fluke surface (Webb 1975; Vogel 1994). Thrust increases with lift until

173   a critical point when the fluke stalls due to the separation of flow from the surface. Thus, the

174   displacement of the *SP* further downstream on the fluke section impedes the separation of flow

175   by extending the favorable pressure gradient. However, downstream displacement of *SP* will

176   foster separation, particularly when the section is canted at an angle to the flow. Mean *SP* values

177   ranged from 0.29 to 0.38 for females and male values ranged from 0.27 to 0.36. Female narwhals

178   had a higher *SP* than male narwhals (Fig. 5), indicating that *SP* was placed further downstream

179   on the fluke section.

180   Male narwhals had lower *TR* values when compared to female narwhals. Average *TR*

181   values for male narwhals ranged from 0.195 to 0.285, while female narwhals ranged from 0.207

182   to 0.442. Streamlined foil sections have lower drags with low *TR* values than high *TR* foils

183   (Abbott and von Doenhoff 1959). Low *TR* foils have a small pressure gradient magnitude, which

184 reduces drag (Fish 2007). Conversely, as the *TR* values increase, as observed in female narwhals,

185 lift is enhanced and stall is delayed. This hydrodynamic performance would be possible because

186 the shape of the cross-section would allow the flow of water to move smoothly over the fluke

187 surface. Similarly, a high *SP* value leads to delayed stall. Consequently, it would appear that the

188 flukes of male narwhals have a hydrodynamic advantage in reducing drag; however, the cross-

189 sectional design of the flukes of female narwhals would tend to increase lift and delay stall.

190   Other limiting factors of induced drag include the sweep of a fluke (Fish 1998b). Female

191 narwhals have a greater sweepback in fluke planform compared to males. Sweepback of a wing

192 or hydrofoil can reduce the induced drag (*i.e.*, drag due to lift) by as much as 8.8% compared to a

193 wing without sweepback (van Dam 1987). Swept back wings produce maximum lift generation

194 at high angles of attack (Fish 1998b). This would be advantageous particularly at low swimming

195 speeds when the angle of attack of the flukes is high (Fish 1993). However, low sweep angles

196 allow for high-efficiency, rapid swimming (Azuma 1983). Based on this information, it is

197 deduced that females would have increased lift but at low swimming speeds, whereas males

198 would have high efficiency at higher swimming speeds.

199   The hydrodynamic effects produced from differences in the geometries of the flukes,

200 which were stated above, are largely associated with steady flow conditions. The flukes of

201 cetaceans are oscillated incurring the dominance of unsteady flow conditions (Webb 1975; Fish

202 1993, 1998a). Unsteady effects can incur lower lift than for steady motion (Lighthill 1970).

203 Further analysis of narwhal fluke geometry would require examination of unsteady effects,

204 although results based on steady flow conditions can provide an indication of differences in

205 hydrodynamic performance.

206   The differences in fluke design between the sexes of narwhals could have hydrodynamic

207   consequences associated with swimming performance. No differences in swimming speeds

208   between male and female narwhals have been reported, when transiting between locations as

209   during migrations (Dietz *et al.* 1995, Dietz *et al.* 2001, Heide-Jørgensen *et al.* 2002, 2003).

210   However, Laidre *et al.* (2003) found that female narwhals made more dives to deeper depths than

211   males. Deeper destination depths were related to increased swimming speed (Laidre *et al.* 2003),

212   indicating that at least during foraging dives, females could be swimming faster than males. The

213   design of the flukes of females, thus, may be associated with the need to transit to greater depths

214   at fast speed. For males, the increased lift and concomitant thrust production from the low

215   sweepback fluke design may aid in compensating for the increased drag that might accompany

216   the possession of the elongate tusk. Swimming performance by narwhals (i.e., overcoming

217   drag, swimming speed) is associated with the hydrodynamically complex and conflicting

218   relationships of lift and thrust production, reduction in drag, delay in stall, and efficiency,

219   which are dependent on the fluke geometry and kinematics.

220

234

LITERATURE CITED

236   Abbott, I. H., and A.E. von Doenhoff. 1959. Theory of Wing Sections. Dover, NY.

237   Azuma, A. 1983. Biomechanical aspects of animal flying and swimming. Pages 35-53 *in*: H.

238   Matsui and K. Kobayashi, eds. Biomechanics VIII-A: International Series on

239   Biomechanics*,* Volume 4A. Human Kinetics Publishers, Champaign, IL.

240   Bose, N., J. Lien, and J. Ahia. 1990. Measurements of the bodies and flukes of several cetacean

241   species. Proceedings of the Royal Society of London B 242: 163-173.

242   Chopra, M.G. and T. Kambe. 1977. Hydrodynamics of lunate-tail swimming propulsion. Part 2.

243   Journal of Fluid Mechanics 79: 49-69.

244   Dietz, R., and M.P. Heide-Jørgensen, 1995. Movements and swimming speed of narwhals

245   (*Monodon monoceros*) instrumented with satellite transmitters in Melville Bay,

246   Northwest Greenland. Canadian Journal of Zoology 73: 2106-2119.

247   Dietz, R., M.P. Heide-Jørgensen, P. Richard, and M. Acquarone. 2001. Summer and fall

248   movements of Narwhals (*Monodon monoceros*) from Northeastern Baffin Island towards

249   Northern Davis Strait. Arctic 54: 246-263.

250   Fish, F.E. 1993. Power output and propulsive efficiency of swimming bottlenose dolphins

251   (*Tursiops truncatus*). Journal of Experimental Biology 185: 179-193.

252 Fish, F.E. 1998a. Comparative kinematics and hydrodynamics of odontocete cetaceans:

253   morphological and ecological correlates with swimming performance. Journal of

254   Experimental Biology 201: 2867-2877.

255 Fish, F.E. 1998b. Biomechanical perspective on the origin of cetacean flukes. Pages 303-324 *in*:

256   J. Thewissen, ed. The Emergence of Whales: Evolutionary Patterns in the Origin of

257   Cetacea. Plenum Press: New York.

258 Fish, F. E., M.K. Nusbaum, J.T. Beneski, and D.R. Ketten. 2006. Passive cambering and flexible

259   propulsors: cetacean flukes. Bioinspiration and Biomimetics 1: S42-S48.

260 Fish, F.E., J.T. Beneski, and D.R. Ketten. 2007. Examination of the three-dimensional geometry

261   of cetacean flukes using computed tomography scans: hydrodynamic implications. The

262   Anatomical Record 290: 614-623.

263 Hay, K., and A. Mansfield. 1989. Narwhal *Monodon monoceros* Linnaeus, 1758. Pages 145-176

264   *in*: S.H. Ridgway, and R. Harrison, eds. Handbook of Marine Mammals. Vol. 4.

265   Academic Press: San Diego, CA.

266 Heide-Jørgensen, M.P. 2009. Narwhal, *Monodon monoceros*. Pages 754-758 *in*: W.F. Perrin,

267   J.G.M. Thewissen, and B. Würsig, eds. Encyclopedia of Marine Mammals. Elsevier, San

268   Diego, CA.

269 Heide-Jørgensen, M. P., R. Dietz, K. L. Laidre, and P. Richard. 2002. Autumn movements, home

270   ranges, and winter density of narwhals (*Monodon monoceros*) tagged in Tremblay Sound,

271   Baffin Island. Polar Biology 25: 331-341.

272 Heide-Jørgensen, M. P., R. Dietz, K. L. Laidre, P. Richard , J. Orr, and H. C. Schmidt. 2003. The

273   migratory behaviour of narwhals (*Monodon monoceros*). Canadian Journal of Zoology

274   81: 1298-1305.

275   Hoerner, S. 1965. Fluid-dynamic drag. Published by author: Brick Town, NJ: Hoerner.

276   Hurt, H., Jr. 1965. Aerodynamics for naval aviators. US Navy, NAV-WEPS 00-80T-80.

277   Department of the Navy: Washington, DC.

278   Laidre, K.L., M.P. Heide-Jørgensen, R. Dietz, R.C. Hobbs, and O.A. Jørgensen. 2003. Deep-

279   diving by narwhals *Monodon monoceros:* differences in foraging behavior between

280   wintering areas? Marine Ecology Progress Series 261: 269-281.

281   Lang, T. 1966. Hydrodynamic analysis of dolphin fin profiles. Nature 209: 1110-1111.

282   Lighthill, J. 1970. Aquatic animal propulsion of high hydromechanical efficiency. Journal of

283   Fluid Mechanics 44 : 265-301.

284   Liu, P. and N. Bose. 1993. Propulsive performance of three naturally occurring oscillating

285   propeller planforms. Ocean Engineering 20: 57-75.

286   Magnuson, J.J. 1978. Locomotion by scombrid fishes: hydrodynamics, morphology and

287   behaviour. Pages 239-313 *in*: W.S. Hoar and D.J. Randall, eds. Fish Physiology, vol. 7.

288   Academic Press, London, UK.

289   Minasian, S.M., K.C. Balcomb, and L. Foster. 1984. The World's Whales. Smithsonian Books,

290   Washington, DC.

291   van Dam, C.P. 1987. Efficiency characteristics of crescent-shaped wings and caudal fins. Nature

292   325: 435-437.

293   Vogel, S. 1994. Life in Moving Fluids. Princeton University Press, Princeton, NJ.

294   von Mises, R. 1945. Theory of Flight. New York: Dover Publishers.

295   Webb, P. 1975. Hydrodynamics and energetics of fish propulsion. Bulletin of the Fisheries

296   Research Board of Canada 190: 1-158.

297   Weihs, D. 1989. Design features and mechanics of axial locomotion in fish. American Zoologist

298   29: 151-160.

299

300   Table 1. Morphometrics of fluke planforms.

301

SPECIMEN	SEX	BODY LENGTH (m)	FLUKE SPAN (m)	PLANFORM AREA (m^2)	ASPECT RATIO	SWEEPBACK ANGLE (deg)	TUSK LENGTH (m)
N0001	F	3.09	0.71	0.13	3.88	33.7	N.A.
N0002	F	2.98	0.70	0.13	3.63	29.0	N.A.
N0003	M	3.60	0.87	0.19	3.90	16.8	1.00
N0004	M	3.57	0.85	0.19	3.86	24.2	0.44

302

303

304

305

306   Figure Legends

307

308   *Figure 1.* CT topograms illustrating the differences between female (N0001, N0002) and male

309   (N0003, N0004) fluke planforms.

310

311   *Figure 2.* Planform and sectional fluke dimensions. The upper figure shows a fluke planform.

312   The vertical solid lines show the root chords (*RC*) and the chord (*C*) at 50% of the blade span.

313   The blade span extends horizontally from *RC* to the fluke tip and the span is the horizontal

314   distance between fluke tips. The sweep angle (Λ) is the angle subtended from a line at the 25%

315   of *RC* and the horizontal dashed line. The lower figure shows a CT image of a fluke section. The

316   horizontal line (*C*) illustrates the chord at 50% of blade span, the dashed vertical line is the

317   maximum thickness (*T*), and the distance from the leading edge to the maximum thickness is the

318   shoulder (*S*). The line within the circle indicates the leading edge radius (*LER*), which is

319   determined from the radius of the white circle that connects tangent points of the leading edge

320   with the upper and lower surfaces of the section.

321

322   *Figure 3.* Linear measurements of male and female flukes of the chord (*C*; solid circles),

323   maximum thickness (*T*; open squares) and shoulder (*S*; open triangles) as a percentage of the

324   fluke blade span, where 0% is at the root chord and 100% is at the fluke tip.

325

326   *Figure 4.* Thickness ratio (*TR*) as a function of fluke blade span for male (open circles) and

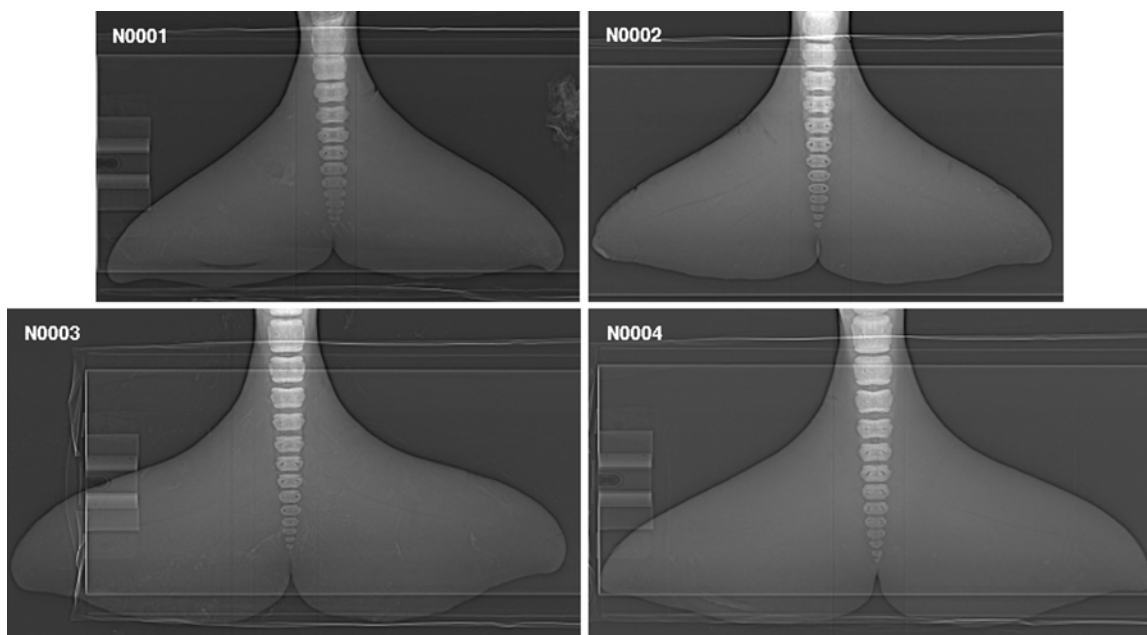327   female (solid circles) narwhals.

328

329   *Figure 5*. Shoulder position (*SP*) of male (open circles) and female (solid circles) narwhals as a

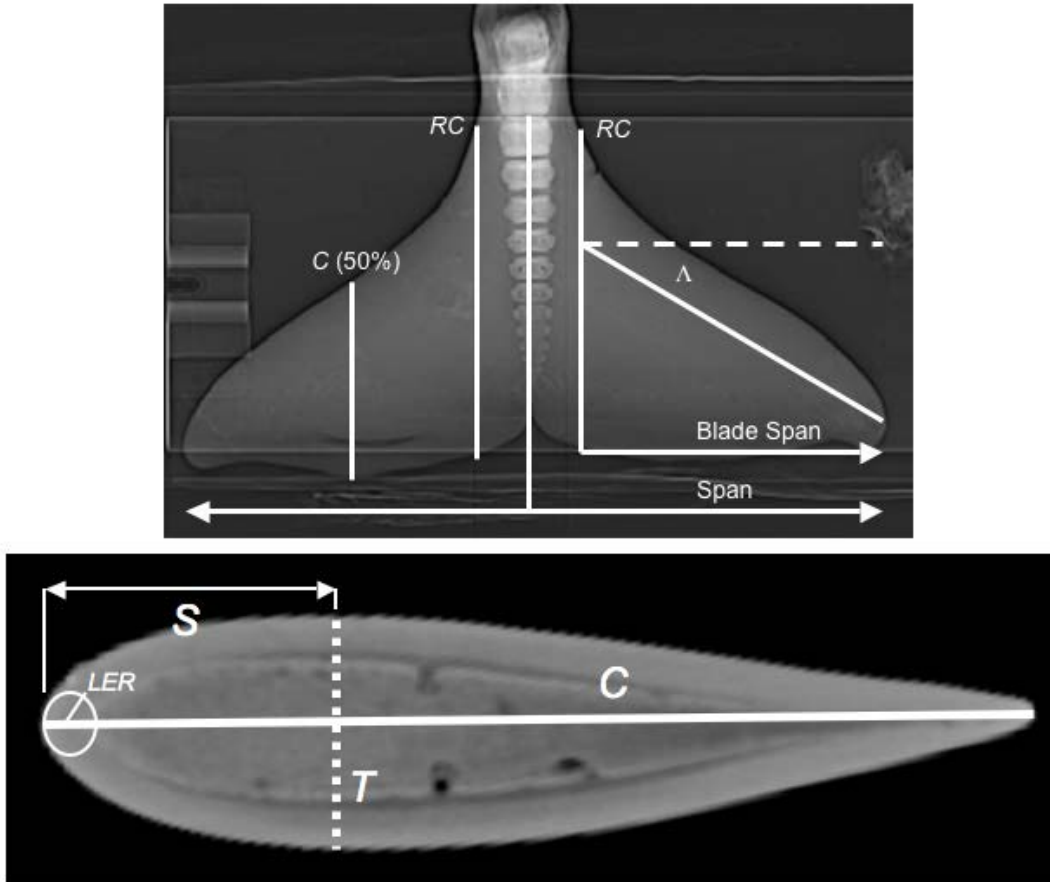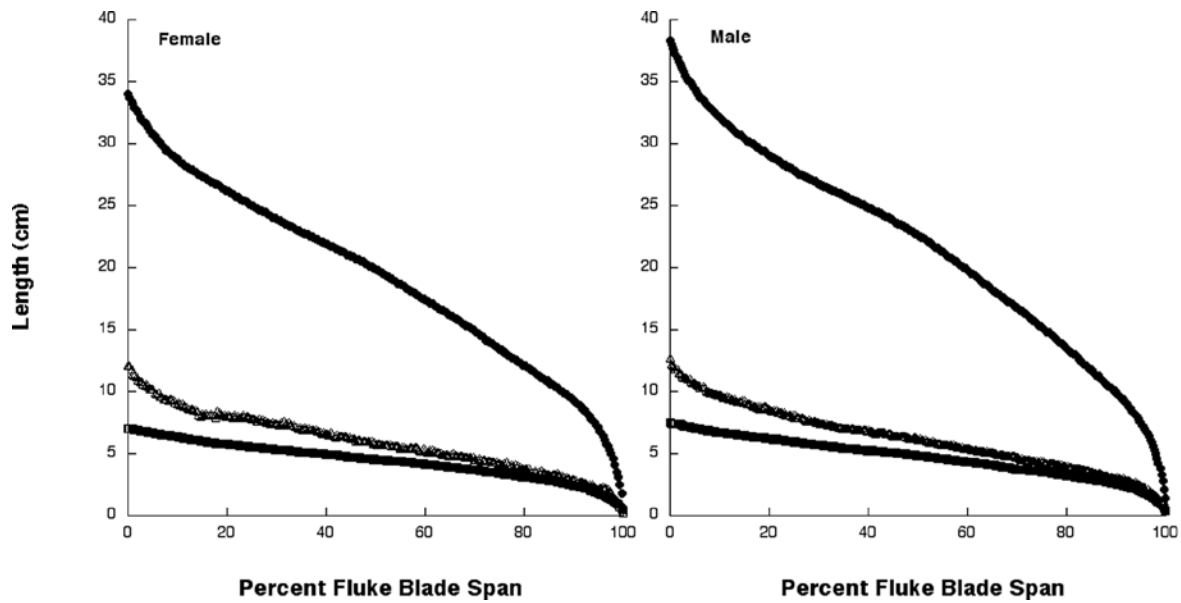330   function of fluke blade span.

331

332

333

334

335

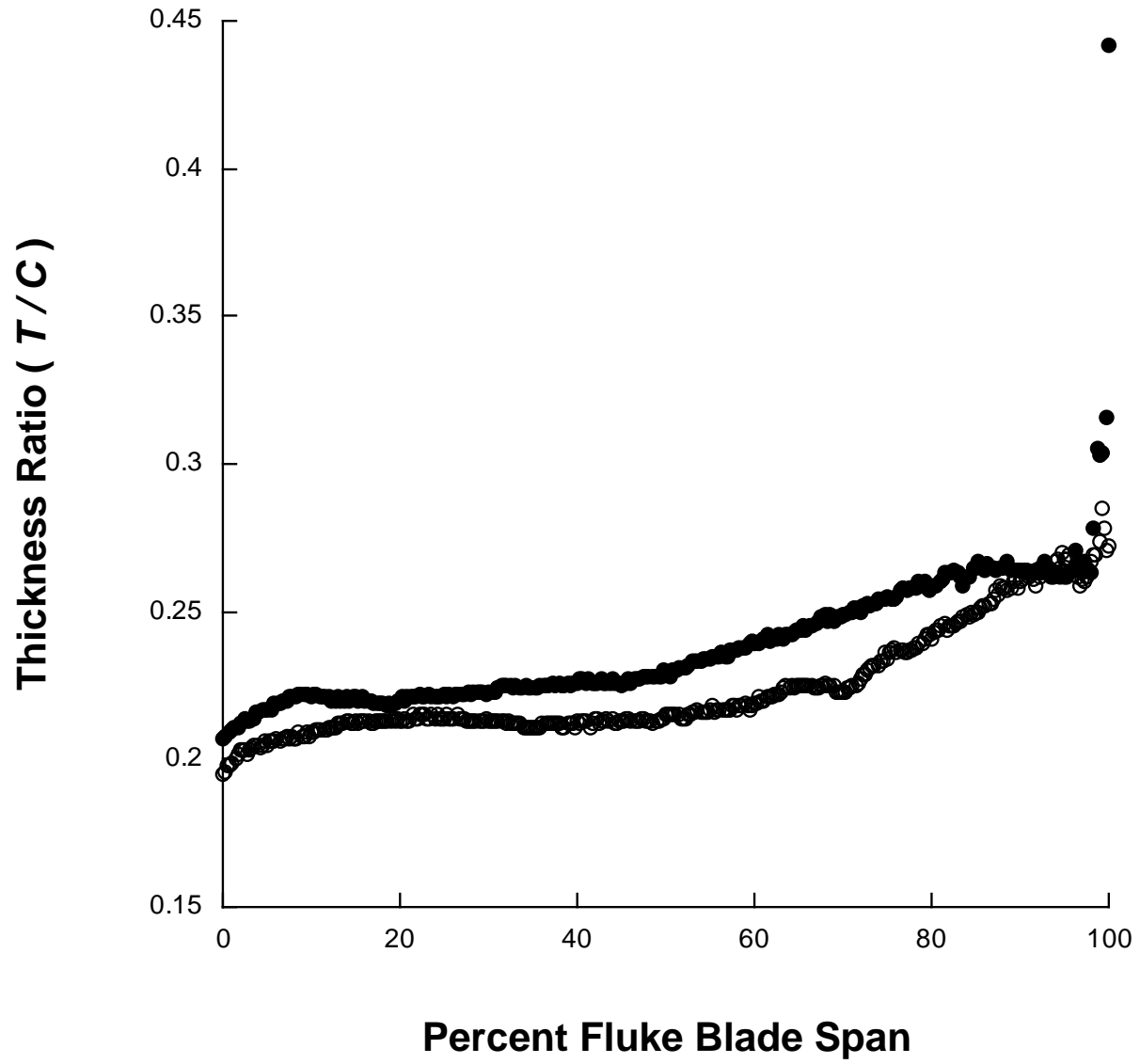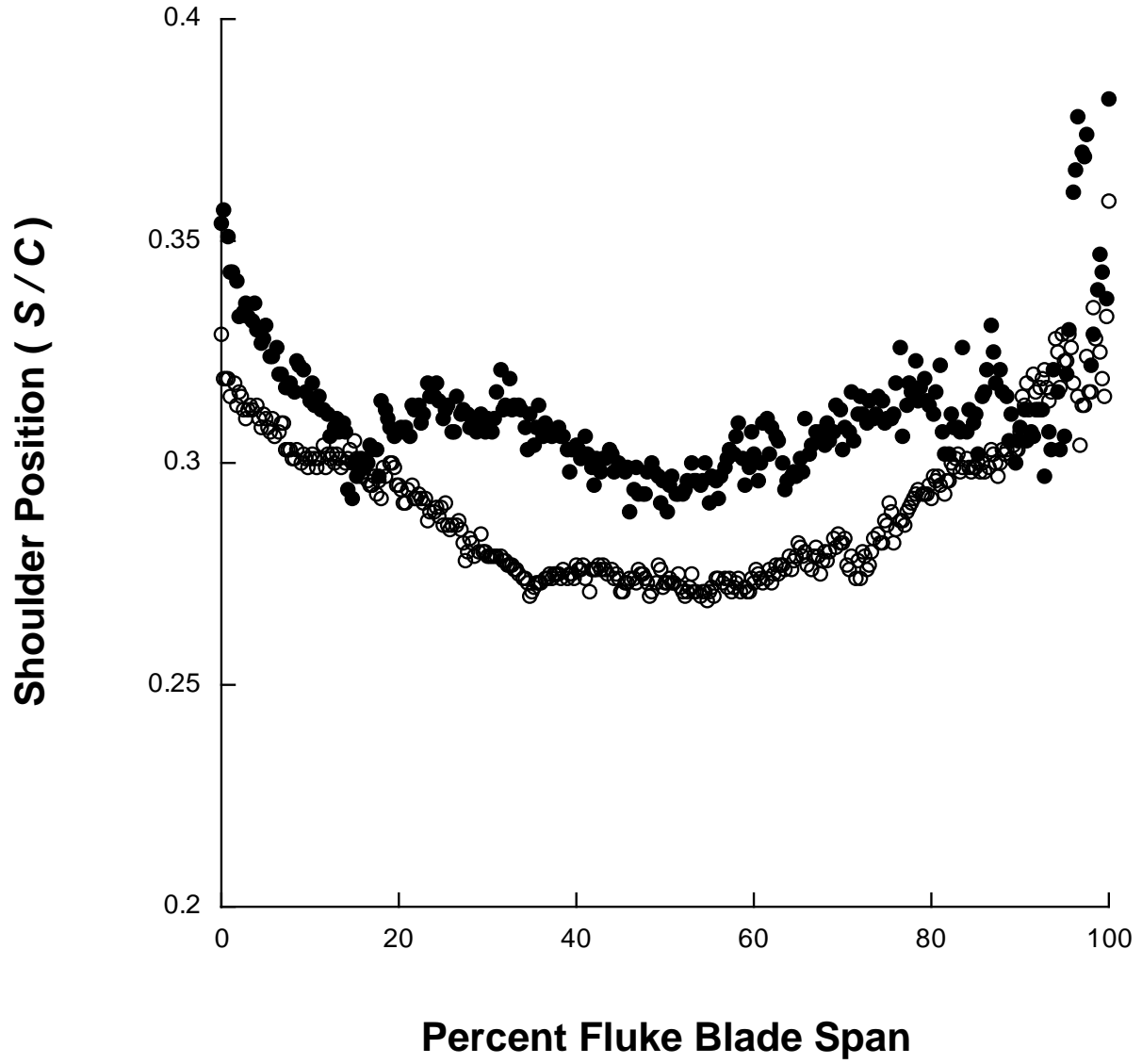336   Figure 1.

337
338   Figure 2.

339

340

341

342   Figure 3.

Figure 4.

346

347

348   Figure 5